OBJECT-ORIENTED CLASSIFICATION OF LIDAR DATA FOR POST-EARTHQUAKE DAMAGE DETECTION

H. Rastiveis[1]*, N. Khodaverdi zahraee[1], A. Jouybari[1]

[1] School of Surveying and Geospatial Engineering, College of Engineering, University of Tehran, Tehran, Iran -
(hrasti, niloofar.zahraee, a.jouybari)@ut.ac.ir

KEY WORDS: LiDAR, Earthquake, Classification, Object Oriented Image Analysis, Buildings Damage Detection

ABSTRACT:

The collapse of buildings during the earthquake is a major cause of human casualties. Furthermore, the threat of earthquakes will increase with growing urbanization and millions of people will be vulnerable to earthquakes. Therefore, building damage detection has gained increasing attention from the scientific community. The advent of Light Detection And Ranging (LiDAR) technique makes it possible to detect and assess building damage in the aftermath of earthquake disasters using this data. The purpose of this paper is to propose and implement an object-based approach for mapping destructed buildings after an earthquake using LiDAR data. For this purpose, first, multi-resolution segmentation of post-event LiDAR data is done after building extraction from pre-event building vector map. Then obtained image objects from post-event LiDAR data is located on the pre-event satellite image. After that, appropriate features, which make a better difference between damage and undamaged buildings, are calculated for all the image objects on both data. Finally, appropriate training samples are selected and imported into the object-based support vector machine (SVM) classification technique for detecting the building damage areas. The proposed method was tested on the data set after the 2010 earthquake of Port-au-Prince, Haiti. Quantitative evaluation of results shows the overall accuracy of 92% by this method.

1. INTRODUCTION

The extraction of building information from high resolution remote sensing data is an important research topic in disaster management studies such as earthquakes, drought, cyclone, etc.(Peng and Liu 2005). Among the mentioned cases, the earthquake is one of the deadliest events that thousands of people are affected every year(Geller 1997). For example, an earthquake that occurred on 12 January 2010 in Port-au-Prince Haiti, killed over 230,000 people and homeless about 1.5 million people.

In case of disaster management after the earthquake, it is important to rapidly identify the building damaged areas, to save people life, and restore the damaged areas(Vetrivel et al. 2015). Initially, the extraction of the damage information can be performed based on the visual interpretation of high-resolution aerial/satellite images. It is an expensive and time-consuming process and difficulty in supporting coherent image interpretation(Rezaeian 2010, Voigt et al. 2007). As an alternative, automatic methods based on image processing algorithms can be used.

Different methods can be used for mapping the building damage area after the earthquake by means of high resolution satellite images, such as comparing the pre- and post-event images(Janalipour and Taleai 2017, Rastiveis, Samadzadegan and Reinartz 2013, Li et al. 2011, Huyck et al. 2005, Miura, Modorikawa and Chen 2011) or based on only post event image(Bai et al. 2017, Zhai et al. 2016, Ishii et al. 2002, Ma and Qin 2012). Most of the studies used both pre-and post-event image data because of their accurate results. But have a major limitation, especially in developing countries, do not have reference data(Li et al. 2011).

Even though optical images are used to extract spectral, textural, shape and morphological properties of buildings, cause several problems such as shadows and high-rise building displacement problems(Rathje et al. 2005, Donnay, Barnsley and Longley 2003). Therefore, Light Detection and Ranging (LiDAR) is employed as a relatively new remote sensing technique rather than spectral information derived from the optical images for building damage detection. Actually, the emergence of LiDAR system makes it possible to acquire accurate height information with low cost and time for identifying damaged and standing buildings. In addition, the data can be acquired independently of lighting conditions and poor illumination such as night, clouds and smoke.

Building damage detection based on LiDAR data is helpful because it is able to collect accurate altitude data immediately after an earthquake and independent of light conditions. Since the LiDAR alone could not be detected all of the buildings, Many studies are based on the comparison of the new LiDAR data with the existing non-LiDAR data such as CAD models, vector maps, and other data as the reference data(Vosselman, Gorte and Sithole 2004, Rehor 2007).

In addition, Most of the studies have worked on building detection, based on the combination of optical imagery and three-dimensional data. This usually improves the building detection results. For example, Vosselman (2004) is detected the differences between building layer of the pre-event vector map and the building image-objects of the LiDAR data for separating building damaged area (Vosselman, Gorte and Sithole 2004). Turker (2005) is used pre and post-event satellite images for generating digital terrain model (DTM) and compared LiDAR height information to distinguish damaged buildings (Turker and Cetinkaya 2005). Turker (2008) is applied shadow for separating building area from post-event image, and compared the results with the pre-event building map to estimate the damage buildings (Turker and Sumer 2008). Chen (2010) is developed a double-threshold strategy

to detect building changes by using old 3D building models and new LiDAR data(Chen and Lin 2010). Awrangjeb(2015) is compared the geographic database with extracted buildings from the newly-available LiDAR data to detect damaged buildings (Awrangjeb 2015). Du (2016) is calculated height difference and grey-scale similarity as change indicators for detecting building changed areas (Du et al. 2016).

The purpose of this study is to develop an object-based method, based on the segment by segment comparison of derived image-objects for building damage detection immediately after the earthquake. For this purpose, this study is organized into four sections. After the introduction, a description of the proposed method for building damage detection is given in Section 2. The experimental area and data are explained in section 3. Finally, implementation results are shown and discussed in section 4.

2. METHODOLOGY

The flowchart of the proposed method summarized in Figure 1. As shown in this figure, first, building areas are extracted on post-event LiDAR data through available pre-event building vector map. In the second step, the image objects are generated through segmentation of LiDAR data. After that, obtained image objects from segmentation are located on the high resolution pre-event satellite image. Then, the proper features that have the higher ability to distinguish building damaged areas from healthy ones are calculated from both data. Finally, building damaged areas are extracted based on selecting appropriate training samples on the study area and importing them to object-based support vector machine classification.
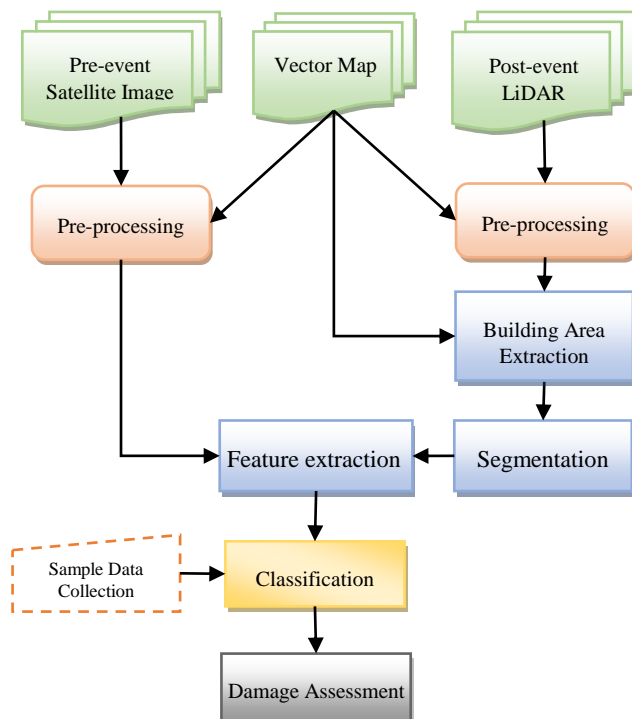

Fig 1. The flowchart of the proposed method for post-earthquake damage assessment using LiDAR data.

2.1 Pre-processing

In some cases, available data from different sources have miss-registration problems such as shift and drift errors. In order to

simultaneously use of these data, accurate co-registration is necessary before any other processing. Therefore, pre-event satellite image and obtained raster image from LiDAR point cloud data are registered with available building vector map in this step. Then, the pre-event image histogram is equalized in order to improve the quality and ease of using it in later stages. Finally, building areas are separated on post-event LiDAR data based on available pre-event building vector map.

2.2 Segmentation

Prior to the building damage detection, the post-event LiDAR data must be segmented for dividing an image into non-overlapping parts and generating meaningful objects (Schiewe 2002). For this purpose, the multi-resolution segmentation is accepted between several segmentation techniques such as split and merge, region growing (Haralick and Shapiro 1985, Pal and Pal 1993). The most important step in data processing is the selection of appropriate segmentation parameters for building damage detection. These parameters include scale, shape, and compactness. In the meantime, the scale represented the size of the object, shape weight, indicated the importance of the spectrum and the compactness weight is represented the importance of the shape. The following equations represent the relationship between these parameters.

$$scale = w_{spectral}.h_{spectral} + w_{shape}.h_{shape}$$

$$w_{spectral} + w_{shape} = 1$$

(1)

$$h_{shape} = w_{compt}.h_{compt} + w_{smooth}.h_{smooth}$$

$$w_{compt} + w_{smooth} = 1$$

(2)

$$h_{compt} = l/\sqrt{n}$$

(3)

$$h_{smooth} = l/b$$

(4)

From these equations, $w_{spectral}$ is spectrum weight, w_{shape} is shape weight, n is the number of pixels, b is the common border length between the object, l is object perimeter, $w_{compact}$ is compactness weight and w_{smooth} is object uniformity.

2.3 Feature extraction

Feature extraction has an important role to capture meaningful information such as shape, texture, spectral and hierarchical from the image objects so it is a critical step in damage detection process. The Purpose of this step is to obtain features that help to detect the damaged buildings. Therefore, an appropriate feature is the one that makes a better difference between damaged buildings and healthy buildings. Based on previous studies, geometry and textural information are useful in damage detection studies(Rastiveis et al. 2013, Janalipour and Mohammadzadeh 2016). In this step of the proposed method, appropriate features should be extracted from both post-event LiDAR data and pre-event satellite image. For this purpose, appropriate features for LiDAR data are extracted immediately after segmentation. But, obtained image-objects

from the LiDAR data are placed on the satellite image and then the image descriptors are extracted. Selected features, for both data including Haralick textural, geometry and statistical features for separating damage buildings are listed in Table 1.

Table1. Applied textural features for change detection

	Feature	Equation
1	GLCM-Homogeneity	$\sum_{i,j=0}^{N-1}\dfrac{p_{i,i}}{1+(i-j)^2}$
2	GLCM-Entropy	$\sum_{i,j=0}^{N-1}p_{i,j}(-\ln p_{i,j})$
3	Max. Diff	$\dfrac{\max\limits_{i,j\epsilon k_B}\left|\overline{c}_i(v)-\overline{c}_j(v)\right|}{\overline{c}(v)}$
4	Standard deviation	$\sqrt{\dfrac{1}{p_v}(\sum\limits_{(x,y,z,t\in p_v)}c_k^2(x,y,z,t)-\dfrac{1}{p_v}(\sum\limits_{(x,y,z,t\in p_v)}c_k(x,y,z,t)^2)}$
5	GLCM-Std. Dev	$\sigma_{i,j}^2=\sum_{i,j=0}^{N-1}P_{i,j}(i,j-\mu_{i,j})$
6	GLCM-Dissimilarity	$\sum_{i,j=0}^{N-1}P_{i,j}\left|i-j\right|$
7	Geometry-Density	$\dfrac{\sqrt{P_v}}{1+\sqrt{\mathrm{var}(X)+\mathrm{var}(Y)}}$
8	Geometry-Compactness	$\dfrac{2\lambda_1\times 2\lambda_2\times 2\lambda_3}{v_v}$
9	Geometry - Asymmetry	$1-\sqrt{\dfrac{\lambda_{\min}}{\lambda_{\max}}}$
10	Brightness	$\overline{c}(v)=\dfrac{1}{w^B}\sum_{K=1}^{K}w_K^B\overline{c}_k(v)$

Haralick features can be calculated using grey-level co-occurrence matrix (GLCM). GLCM is a matrix that contains the number of each grey level pairs that are located at distance d and direction θ from each other(Haralick and Shanmugam 1973).

$$GLCM=\frac{1}{R}\begin{bmatrix}\eta(0,0) & \eta(0,1) & . & \eta(0,N_{g-1})\\ \eta(1,0) & \eta(1,1) & . & .\\ . & . & . & .\\ \eta(N_{g-1},0) & . & . & \eta(N_{g-1},N_{g-1})\end{bmatrix}\quad(5)$$

Form this equation, $\eta(1,0)$ is pixel pairs in lag (di,dj), Ng is the Number of Gray levels and R is the total number of possible pairs

Geometry features are based on the shape of an image object and Statistical features are evaluate the relationship between image objects(Haralick and Shanmugam 1973).

2.4 Classification

This is the most important step in automatic damage detection algorithms from remote sensing data. Traditional pixel-based classification is widely used in change detection applications such as forest and environmental monitoring. However, this method has produced undesirable results in the case of building damage detection. In addition, traditional pixel-based classification cannot differentiate between object features that display high spectral overlap, such as, building roofs from pavements that are constructed using similar material. Furthermore, object-based classification offers possibilities to overcome these problems. This method takes into account knowledge of neighbourhood pixels. The object-oriented method is generally based on the concept that important semantic information is not represented in single pixels alone but in meaningful image-objects and their mutual relations.

There are various methods for image classification. Nowadays the scientist interested in to use SVM in the object-based case because it has much ability with good accuracy as well as the rapid process.

The Support Vector Machine (SVM) is a non-linear approximation that is a method for binary classification. The aim of this algorithm is finding the optimal hyperplane that separates the d-dimensional data with maximum margin into two classes. SVM use kernel feature space that transmits the data into higher dimensional space. Equation 1, show the aim of non-linear SVM.

Let l training samples $\{X_i,\ Y_i\}, i=1...l$ and $(X_i\in R^d)$
Parameterized hyperplanes by a vector $(w)\rightarrow w.x+b=0$
Hyperplane (w,b) that separates the data by a distance +1,-1

$$\left.\begin{array}{l}x_i.w+b\geq 1-\xi_i\quad for\,y_i=1\\ x_i.w+b\leq -1+\xi_i\quad for\,y_i=-1\end{array}\right\}\quad y_i(w.x_i+b)\geq 1-\xi\ (6)$$

For obtaining geometric distance magnitude of w must be normalized by,

$$d((w,b),x_i)=\frac{y_i(x_i.w+b)}{\|w\|}\geq\frac{1}{\|w\|}\qquad(7)$$

Minimizing w by Lagrange multipliers

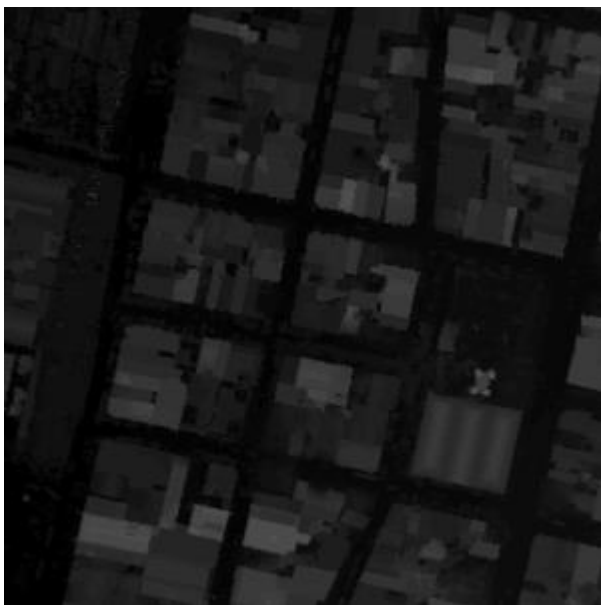$$w(\alpha)=-\sum_{i=l}^{l}\sum_{j=1}^{l}y_iy_j\alpha_i\alpha_j(x_i,x_j)\qquad(8)$$

Optimal hyperplane

$$w=\sum_i\alpha_iy_ix_i\qquad(9)$$

Finally two classes of damaged and undamaged buildings are obtained in this step through object-based SVM algorithm.

3. STUDY AREA

The earthquake on 12 January 2010 near Port-au-Prince, Haiti, killed over 230,000 people and caused extensive damage in

Port-au- Prince. Because of the high density of collapsed and damaged structures the 2010 Haiti earthquake is an ideal case study to evaluate automated damage detection methods. For this research, we obtained high resolution pre-earthquake satellite image and LiDAR point cloud data. A pre-disaster satellite image was acquired on 1 October 2009 by the WorldView-2 satellite and post-disaster point cloud was acquired on 15 January 2010 by LiDAR. Figure 2. Depicted the selected area from the data set. This area represents densely built-up areas comprising multi-story buildings, urban vegetation, and roads partly covered by debris.

Fig 3. Used building vector map

4. TEST AND EVALUATION

In order to easily detect building damage area, first building areas were distinguished on post-event LiDAR data by a pre-event building vector map. Figure 4. Demonstrates extracted building area on post-event LiDAR data by pre-event building vector map.

(a)

(b)

Fig 2. Selected area from the data set as test area. a) Post-event LiDAR. b) High resolution pre-event satellite image

Pre-event vector map from study area are used for building area extraction. Figure 3. Represents the used pre-earthquake building vector map in pre-processing step.
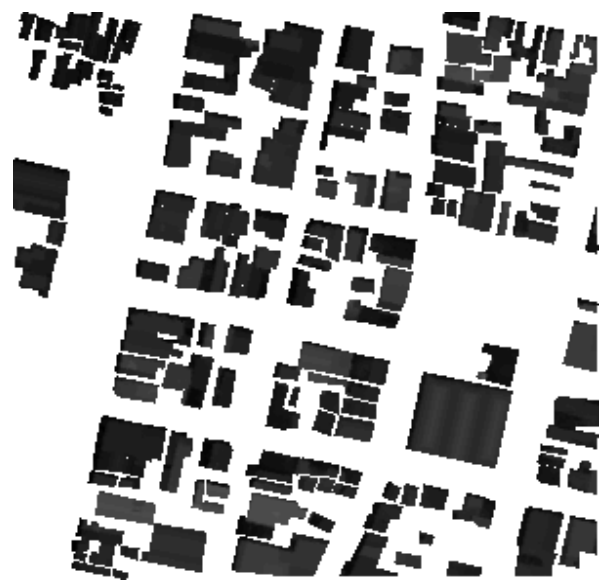

Fig 4. Extracted building area by pre-event building vector map on post-earthquake LiDAR data

After data pre-processing, segmentation of LiDAR data was implemented through multi-resolution segmentation algorithm. Required parameters such as shape, scale, and compactness were equal to 15, 0.3 and 0.7 for the LiDAR data. Figure 5. Demonstrates the LiDAR segmented image using mentioned parameters.
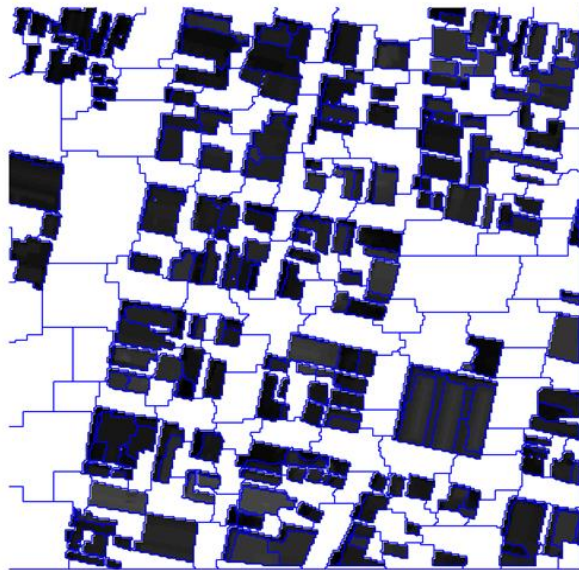
Fig 5. LiDAR, segmented image through multi-resolution segmentation algorithm

Obtained image-objects from segmentation of LiDAR data are placed on pre-event satellite image and suitable features are calculated from both of Lidar and satellite image. Figure 6. Demonstrates the obtained image objects from LiDAR data on pre-event satellite image.
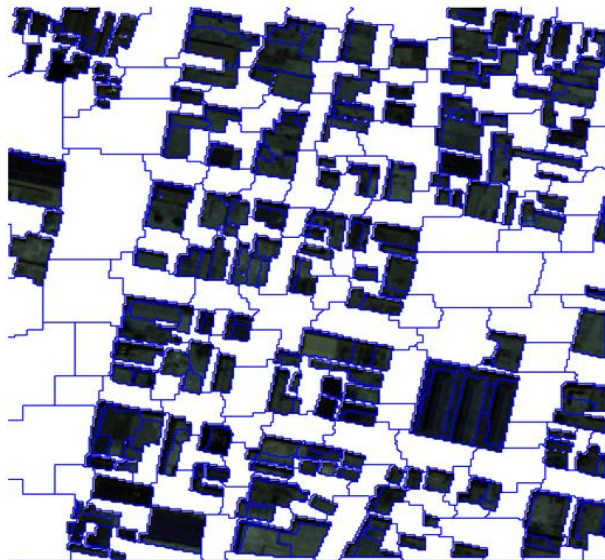

Fig 6. Obtained image objects from LiDAR data on pre-event satellite image.

Besides, 46 image objects including extracted features from the pre-event image and post-event LiDAR data were observed manually to be used for training the object-based SVM. Linear kernel function with control parameter (C) 1 is selected for classifying the post-event LiDAR data using SVM classification algorithm. Figure 7 shows the classification result on post-earthquake LiDAR data in two classes of damaged and undamaged.
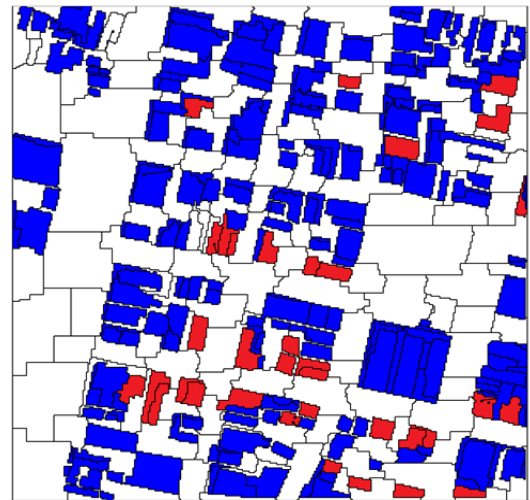

Fig 7. SVM's output in two classes: Red polygon shows damaged buildings and blue shows healthy buildings.

As seen in Figure 7, red polygons show damaged area and blue areas show healthy buildings. SVM's confusion matrix for this classification is shown in Table 3. As can be seen in Table 3, among 37 manually observed image objects as test data, the proposed algorithm detected 20 correct undamaged image object and 14 correct building damaged image object, and obtained overall accuracy by proposed method is 92%.

Table 3. SVM's confusion matrix

	undamaged	damaged
undamaged	20	2
damaged	2	14
Overall accuracy=92%		

5. CONCLUSION

In this paper, a new method for mapping damaged buildings after an earthquake using LIDAR data and pre-event high-resolution satellite image was proposed and implemented. The pre-event vector map is used for separating building area as an ancillary data.

By means of the multi-resolution method and appropriate selection of parameters including shape, compactness, and scale, the segmentation was done on LiDAR data. Homogeneity, Entropy, Max. Diff, Std. Dev, Ang.2nd Moment, dissimilarity, compactness, brightness, density, and asymmetry information were extracted from both data. Finally, selected training samples were applied as an input feature vector in a object-based support vector machine (SVM) for classifying the area into two classes of damaged and undamaged buildings. The obtained overall accuracy, 92%, showed the ability of the proposed technique for distinguishing destroyed buildings from healthy buildings. Also, the classification results indicate that it is useful to use the pre-event image beside the LiDAR data in order to building damage detection. Although the results, especially in comparison with manually observed image objects, were promising, however, further studies need to improve the results.

REFERENCES

Bai, Y., B. Adriano, E. Mas, H. Gokon & S. Koshimura (2017) Object-Based Building Damage Assessment Methodology Using Only Post Event ALOS-

2/PALSAR-2 Dual Polarimetric SAR Intensity Images. *Journal of Disaster Research Vol,* 12**,** 259.

Donnay, J.-P., M. J. Barnsley & P. A. Longley. 2003. *Remote sensing and urban analysis: GISDATA 9*. CRC Press.

Ferreira, J. & A. Bernardino. 2006. Acquisition of 3D regular prismatic models in urban environments from DSM and orthoimages. In *CompIMAGE*, 185-190.

Forlani, G., C. Nardinocchi, M. Scaioni & P. Zingaretti (2006) Complete classification of raw LIDAR data and 3D reconstruction of buildings. *Pattern Analysis and Applications,* 8**,** 357-374.

Geller, R. J. (1997) Earthquake prediction: a critical review. *Geophysical Journal International,* 131**,** 425-450.

Haralick, R. M. & K. Shanmugam (1973) Textural features for image classification. *IEEE Transactions on systems, man, and cybernetics***,** 610-621.

Haralick, R. M. & L. G. Shapiro (1985) Image segmentation techniques. *Computer vision, graphics, and image processing,* 29**,** 100-132.

Huyck, C. K., B. J. Adams, S. Cho, H.-C. Chung & R. T. Eguchi (2005) Towards rapid citywide damage mapping using neighborhood edge dissimilarities in very high-resolution optical satellite imagery—Application to the 2003 Bam, Iran, earthquake. *Earthquake Spectra,* 21**,** 255-266.

Ishii, M., T. Goto, T. Sugiyama, H. Saji & K. Abe. 2002. Detection of earthquake damaged areas from aerial photographs by using color and edge information. In *Proceedings of the Fifth Asian Conference on Computer Vision*, 27-32.

Janalipour, M. & A. Mohammadzadeh (2016) Building damage detection using object-based image analysis and ANFIS from high-resolution image (Case study: BAM earthquake, Iran). *IEEE Journal of Selected Topics in Applied Earth Observations and Remote Sensing,* 9**,** 1937-1945.

Janalipour, M. & M. Taleai (2017) Building change detection after earthquake using multi-criteria decision analysis based on extracted information from high spatial resolution satellite images. *International Journal of Remote Sensing,* 38**,** 82-99.

Li, H., H. Gu, Y. Han & J. Yang. 2007. Fusion of high-resolution aerial imagery and lidar data for object-oriented urban land-cover classification based on svm. In *ISPRS Workshop on Updating Geo-spatial Databases with Imagery & The 5th ISPRS Workshop on DMGISs*.

Li, X., W. Yang, T. Ao, H. Li & W. Chen (2011) An improved approach of information extraction for earthquake-damaged buildings using high-resolution imagery. *Journal of Earthquake and Tsunami,* 5**,** 389-399.

Ma, J. & S. Qin. 2012. Automatic depicting algorithm of earthquake collapsed buildings with airborne high resolution image. In *Geoscience and Remote Sensing Symposium (IGARSS), 2012 IEEE International*, 939-942. IEEE.

Miura, H., S. Modorikawa & S. H. Chen. 2011. Texture characteristics of high-resolution satellite images in damaged areas of the 2010 Haiti earthquake. In *Proceedings of the 9th International Workshop on Remote Sensing for Disaster Response, Stanford, CA, USA*, 15-16.

Oczipka, M., T. Bucher & A.-M. Trosset (2008) Mapping and updating maps in dense urban regions using high resolution digital airborne imagery, surface models

and object-based classification. *IAPRS, Beijing 2008,* 37**,** 551-555.

Pal, N. R. & S. K. Pal (1993) A review on image segmentation techniques. *Pattern recognition,* 26**,** 1277-1294.

Peng, J. & Y. Liu (2005) Model and context-driven building extraction in dense urban aerial images. *International Journal of Remote Sensing,* 26**,** 1289-1307.

Rastiveis, H., F. Samadzadegan & P. Reinartz (2013) A fuzzy decision making system for building damage map creation using high resolution satellite imagery. *Natural Hazards and Earth System Sciences (NHESS),* 13**,** 455-472.

Rathje, E. M., K.-S. Woo, M. Crawford & A. Neuenschwander. 2005. Earthquake damage identification using multi-temporal high-resolution optical satellite imagery. In *Geoscience and Remote Sensing Symposium, 2005. IGARSS'05. Proceedings. 2005 IEEE International*, 5045-5048. IEEE.

Rehor, M. (2007) Classification of building damage based on laser scanning data. *The Photogrammetric Journal of Finland,* 20**,** 54-63.

Rezaeian, M. 2010. *Assessment of earthquake damages by image-based techniques*.

Rottensteiner, F., J. Trinder, S. Clode & K. Kubik. 2003. Building detection using LIDAR data and multispectral images. In *Digital Image Computing: Techniques and Applications*, 673-682. CSIRO.

Schiewe, J. (2002) Segmentation of high-resolution remotely sensed data-concepts, applications and problems. *International Archives of Photogrammetry Remote Sensing and Spatial Information Sciences,* 34**,** 380-385.

Turker, M. & E. Sumer (2008) Building-based damage detection due to earthquake using the watershed segmentation of the post-event aerial images. *International Journal of Remote Sensing,* 29**,** 3073-3089.

Vetrivel, A., M. Gerke, N. Kerle & G. Vosselman (2015) Identification of damage in buildings based on gaps in 3D point clouds from very high resolution oblique airborne images. *ISPRS journal of photogrammetry and remote sensing,* 105**,** 61-78.

Voigt, S., T. Kemper, T. Riedlinger, R. Kiefl, K. Scholte & H. Mehl (2007) Satellite image analysis for disaster and crisis-management support. *IEEE transactions on geoscience and remote sensing,* 45**,** 1520-1528.

Vosselman, G., B. Gorte & G. Sithole (2004) Change detection for updating medium scale maps using laser altimetry. *International Archives of Photogrammetry, Remote Sensing and Spatial Information Sciences,* 34**,** 207-212.

Xi, Y. & Q. Luo (2018) A morphology-based method for building change detection using multi-temporal airborne LiDAR data. *Remote Sensing Letters,* 9**,** 131-139.

Yu, B., H. Liu, J. Wu, Y. Hu & L. Zhang (2010) Automated derivation of urban building density information using airborne LiDAR data and object-based method. *Landscape and Urban Planning,* 98**,** 210-219.

Yu, B., H. Liu, L. Zhang & J. Wu. 2009. An object-based two-stage method for a detailed classification of urban landscape components by integrating airborne LiDAR and color infrared image data: A case study of downtown Houston. In *Urban Remote Sensing Event, 2009 Joint*, 1-8. IEEE.

Zhai, W., H. Shen, C. Huang & W. Pei (2016) Building earthquake damage information extraction from a single post-earthquake PolSAR image. *Remote Sensing,* 8**,** 171.

Turker, M. & B. Cetinkaya (2005) Automatic detection of earthquake-damaged buildings using DEMs created from pre-and post-earthquake stereo aerial photographs. *International Journal of Remote Sensing,* 26**,** 823-832.

Vosselman, G., B. Gorte & G. Sithole (2004) Change detection for updating medium scale maps using laser altimetry. *International Archives of Photogrammetry, Remote Sensing and Spatial Information Sciences,* 34**,** 207-212.

Awrangjeb, M. (2015) Effective generation and update of a building map database through automatic building change detection from LiDAR point cloud data. *Remote Sensing,* 7**,** 14119-14150.

Chen, L.-C. & L.-J. Lin (2010) Detection of building changes from aerial images and light detection and ranging (LIDAR) data. *Journal of Applied Remote Sensing,* 4**,** 041870.